# High-Arctic glacial-periglacial interactions and the development of terrain morphology on Brøggerhalvøya, Svalbard

TDL Irvine-Fynn,
*Department of Geography, University of Sheffield, Sheffield, South Yorkshire, UK.*
PR Porter,
*Division of Geography and Environmental Sciences, University of Hertfordshire, Hatfield, Hertfordshire, UK.*
NE Barrand,
*Department of Geography, University of Alberta, Edmonton, Alberta, Canada.*
DI Benn, M Temminghoff,
*University Centre in Svalbard (UNIS), PO Box 156, Longyearbyen N-9171, Svalbard, Norway.*
S Lukas
*Department of Geography, Queen Mary University of London, London, UK.*

## ABSTRACT

Recent geodetic analyses for small valley glaciers in western Svalbard have shown sustained, negative mass balance and an accelerating rate of thinning. One consequence of such ice mass loss is the increased exposure of forefield moraine complexes. Such deglaciating areas are susceptible to processes of sediment reworking and redistribution, highlighting that, for beyond century time-scales; even in permafrost environments, the preservation of ice-marginal landforms is limited. Here, a summary of results from three sequential investigations are used to explore the mechanisms involved in morphological terrain adjustment within deglaciating catchments on Brøggerhalvøya, north-west Svalbard. Specifically, the presence of buried ice and exposure of glacial sediments at the ice margins are shown to have significant roles in processes associated with deglaciation.

## RÉSUMÉ

Des analyses géodésiques récentes faites dans des petits glaciers au Spitzberg occidental ont montré que la plupart présente continuellement un bilan de matière négatif et un taux croissant de d'amincissement. L'une des conséquences d'une telle perte de masse est une plus grande exposition des ensembles de moraines frontales. Dans ces secteurs de déglaciation, des processus de remodelage sédimentaires sont possibles. Ceci montre que, à l'échelle de plusieurs siècles, et même dans des environnements de permafrost, la préservation des structures glaciaires marginales est limitée. Dans cette étude, le bilan de trois analyses séquentielles est utilisé pour explorer les mécanismes impliqués dans les ajustements morphologiques du terrain dans les bassins présentant une déglaciation dans la formation du Brøggerhalvøya (nord-ouest du Spitzberg). En particulier, la présence de glaces enfouies et l'exposition de sédiments glaciaires au niveau des fronts glaciaires jouent un rôle important dans les processus liés à la déglaciation.

## 1    INTRODUCTION

Approximately 36000 km$^2$ of Svalbard are currently ice-covered with maximum glacier extents reached around 1900 at the end of the Little Ice Age (LIA; Svendsen and Mangerud, 1997). Subsequently, between 1936 and 1990, there has been a 16% reduction in the region's glaciated area corresponding to an average geodetic glacier thinning rate of –0.3m/a, with evidence of accelerating ice loss in more recent years (Kohler et al., 2007; Nuth et al., 2007). Locally, over the same timeframe, this deglaciation has reduced ice areas by up to 45% and equate to 50 m declines in glacier surface elevation (e.g. Ziaja, 2001). Such environmental changes have resulted in the progressive exposure of glacial moraines, diamicts and tills at the ice margins. In receeding, most land-terminating glaciers have left moraine ridges at the location of their maximum LIA extent (Hagen et al., 1993) with evidence of inactive buried ice and ice-cored moraines in proglacial areas

(Etzelmüller, 2000; Gibas et al., 2005; Hoelzle, 1993; Schomacker and Kjær, 2008) and opening ice marginal zones to increasing fluvial and periglacial processes of terrain modification (Etzelmüller and Hagen, 2005; Etzelmüller et al., 2000; Lønne and Lyså, 2005; Lukas et al., 2005).

Here, a suite of studies utilizing remote sensing techniques combined with field observations are employed to better understand processes involved in deglaciating catchments in Svalbard. With focus on the Brøggerhalvøya peninsula in north-western Svalbard, two sequential catchment-scale airborne lidar surveys are used to explore contemporary rates and proglacial terrain change; unique drainage configuration coupled with time-lapse imagery highlights processes operating at a deglaciating ice margin; and digital elevation models (DEMs) coupled with resistivity surveys provide an estimate of the areal extent of proglacial-periglacial sedimentary structures and relation to landscape relaxation. These studies enable confirmation of hitherto

conceptual models of landscape change by providing quantification and characterization of the mechanical processes involved, allowing inferences of their morphological significance to be made.

## 2    STUDY SITE

Brøggerhalvøya is a glaciated peninsula located in the north-west of Svalbard (78.9°N 11.8°E; Figure 1) and geologically is characterised by Paleozoic sedimentary and Proterozoic metamorphic rocks thrust above sedimentary Tertiary formations (Svendsen et al., 2002). With mean annual air temperatures of –6.1°C at sea level (Førland et al., 1997), permafrost in the area ranges between 140 and 450 m depth (Liestøl, 1976) with an active layer depth typically < 1.5 m (Hallet and Prestrud, 1986). The local geomorphology is conditioned by glacial activity, with large moraine complexes developed during the LIA ice advance comprising contemporary and older material (Hjelle et al., 1999). Previous studies have suggested buried ice within the moraines is widespread in the region (Hambrey, 1984; Hoelzle, 1993). The northeast facing portion of the peninsula contains a series of sub-parallel, land-terminating, alpine valley glaciers at varying stages of retreat form their LIA maxima (Glasser and Hambrey, 2001). Seasonally active streams aid in the reworking of glacial sediments, emerging from the moraine complexes and flowing over wide, coarse-deposit sandar prior to reaching the fjord (Mercier and Laffly, 2005; Svendsen et al., 2002).
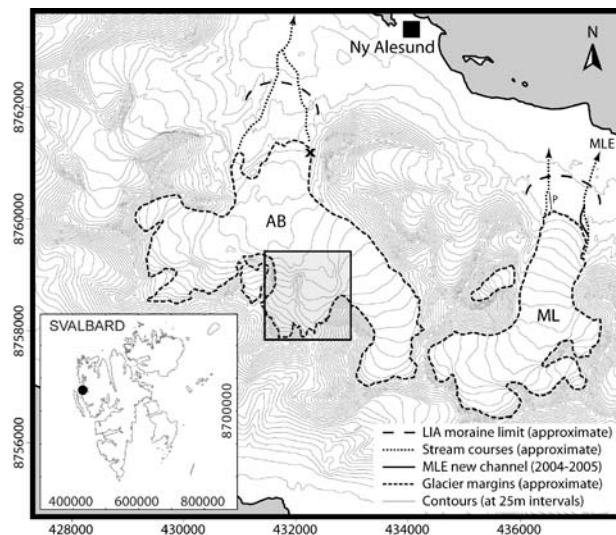


Figure 1. Map of location of Brøggerhalvøya (inset) and details of AB and ML in UTM projection (Zone 33N). Contemporary glacier margins, proglacial streams, and LIA moraine limits are shown. Stream channel change along MLE is indicated with a solid line and the englacial portal at AB is indicated with 'x'. Location of the profile discussed in Figure 4 is indicated by 'P'. The shaded area on AB is the region in which debris flows reaching the ice surface were observed and monitored.

The study presented here focuses upon the catchments of two north-facing glaciers: Austre Brøggerbreen (AB) and Midtre Lovénbreen (ML), with respective areas of 10.2 and 5.1 km$^2$ in 2005 (Figure1; Barrand et al., 2010). Midtre Lovénbreen has a polythermal regime evidenced by radar soundings (Björnsson et al., 1996; Rippin et al., 2003), while AB was predominantly cold-based (Björnsson et al., 1996) but is now thought to be entirely cold-based due to its recent thinning (Glasser and Hambrey, 2001; Hodson et al., 2002).

Both glaciers have maximum elevations ~ 600-650 m above sea level (masl) and field-based analyses have shown protracted negative mass balance, with averages of –0.49 and –0.39 m water equivalent (w.e.) for AB and ML, respectively, between 1967 and 2006 (J Kohler, pers. comm.). More recent geodetic estimates of ice mass loss, while showing the same trends, suggest that the field-based analysis may underestimate true thinning rates by up to 17% (Barrand et al., 2010). Both ML and AB termini have exhibited lateral retreat of the order of 1 km since the LIA associated with the negative mass balances. Such retreat has exposed large areas of poorly consolidated, mainly coarse diamict which can be reworked by periglacial, fluvial and slope processes and has spatially discontinuous pioneer plant colonization and disturbance (Moreau et al., 2008). Proglacial streams in the forefield commence at the eastern and western limits of both glaciers and flow north through the LIA moraine limits and across large braided sandur areas (Figure 1).

Despite the geomorphological and ecological interest in newly exposed forefields, and the existing awareness of the likelihood of buried ice forms at locations on Brøggerhalvøya (e.g. Etzelmüller, 2000; Hoelzle, 1993), the local rates of morphological terrain change remain poorly understood especially with regard the processes of sediment mobilization and spatial significance of buried ice forms.

## 3    ANALYTICAL CASE STUDIES: METHODS AND RESULTS

Because the results presented here, while focused upon similar research questions, use three distinct investigative techniques, the methods and results for each are presented sequentially below.

### 3.1    Insights from Lidar Difference Models

To assess contemporary processes and rates of forefield terrain change, two sequential lidar surveys were compared to field-based observations made at ML.

#### 3.1.1    Lidar difference model

During 2003 (Aug 9th) and 2005 (July 5th), two basin-scale airborne lidar surveys were completed to provide high-resolution elevation data sets. Data were collected using an Optech ALTM3033 laser scanner with a scanning rate of 13 Hz yielding a point sample density of 1 per 1.83 m$^2$. Data density varies due to geometric conditions and scanning swath overlaps: the spatial resolution of the

entire forefield dataset is calculated as 1.10 point per m$^2$, with a vertical resolution of ±0.14 m. For full details of the lidar data collection refer to Barrand et al (2009). Digital elevation models (DEMs) were created with 1 m horizontal resolution using a Delauney triangulation gridding algorithm.

To assess morphometric change over time, a raster difference layer was created by subtracting the 2003 and 2005 DEMs. The difference raster was clipped to the area of the forefield alone, and patches of standing water, icing and snow were identified and removed using orthorectified aerial photographs collected simultaneously with the lidar surveys.

Figure 2 presents the processed DEM difference model. Note the two key areas of change: the eastern stream reach and the western ridge, respectively evidencing change by fluvial and periglacial processes. The rates of change for these isolated areas are shown in Table 1, assuming representativeness of the 23 months elapsed between surveys.
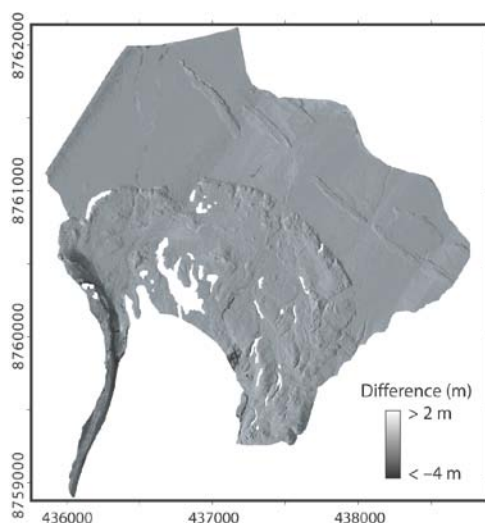


Figure 2. Map DEM difference from 2003 and 2005 lidar data sets. Note the regions of large change (lowering in excess of 2m): the western moraine ridge and the newly incised MLE channel near the glacier centre-line close to the snout. Map is projected in UTM WGS84.

Table 1. Proglacial change detected using lidar surveys.

| Location | Area (km$^2$) | Elevation change (ma$^{-1}$) | Volume change (×10$^5$ m$^3$) |
|---|---|---|---|
| Forefield | 4.66 | −0.05 ±0.2 | −4.59 ±9.32 |
| Active east channel | 0.04 | −0.13 ±0.2 | −0.02 ±0.09 |
| Western ridge | 0.17 | −0.65 ±0.2 | −2.19 ±0.34 |

The moraine ridge, with lowering of around 0.7 ma$^{-1}$ compares well to published values of vertical ice-cored terrain degradation on Svalbard (e.g. Etzelmüller, 2000; Lukas et al., 2005; Schomacker and Kjær, 2008). Fluvial action at locations along the moraine, and mass failure of

the debris mantle (Figure 3a) clearly showed the ice-core extended for the majority of the ridge's elevation range. The lowering rate of 0.05 ma$^{-1}$ over the remaining proglacial area suggested other portions of the forefield were also ice-cored. Such lowering is suggestive or reworking processes and landscape degradation resulting from thermal erosion of underlying ice bodies.
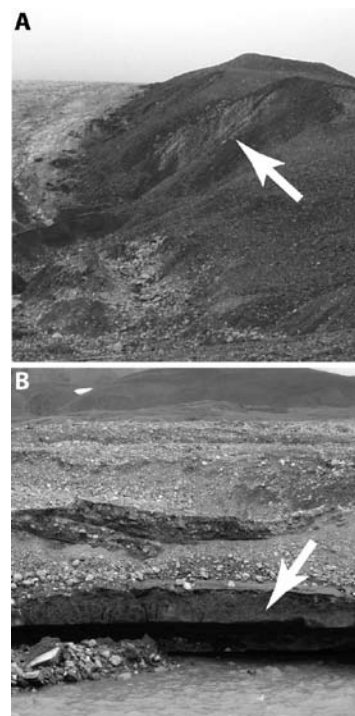


Figure 3. Images showing (A) mass failure (slumping) exposing the ice core of the moraine ridge at the western margin of ML and (B) exposure of buried ice by fluvial incision of new (2004) MLE channel in the ML forefield.

### 3.1.2 Comparisons between field data and lidar difference

The lidar difference model highlighted two key mechanical processes involved with the degradation of the ML forefield: fluvial and periglacial degradation. As noted above, the eastern proglacial stream reach and ridge emergent at the western flank of the glacier showed the most significant elevation change over the 23 months between the lidar surveys. To explore these changes in more depth, field observations were also examined.

During the 2004 melt season, between the lidar surveys, hydrological data including discharge (Q) and in-stream suspended sediment concentration (SSC) were collected at all sites where meltwater drained from the ML catchment through the LIA moraine limit (Figure 1). Standard methods were used (e.g. Hodson and Ferguson, 1999) with probabilistically determined errors in Q and SSC of < 19% and < 26%, respectively. In 2004, the emergence of turbid waters characteristic of subglacial waters at a polythermal glacier occurred at a portal on the western side of the ML snout. This situation ensured that the sediment load monitored in the eastern

stream was of proglacial origin only. Moreover, during 2004, observations showed the eastern stream exhibited significant adjustment of its course (Figure 1), as highlighted in the lidar difference model. Taking typical moraine density of between 1.5 – 2.0 g/cm$^3$, the topographic change along the eroded reach of MLE identified by lidar equates to between 3000 and 4000(±18000) ×10$^3$kg.

Over the 2004 monitoring period sediment yield from the eastern stream was calculated to be 1100(±370) ×10$^3$kg from the records of Q and SSC. This value was adjusted to 1600(±570) ×10$^3$kg by assuming observations occurred over only 70% of the active hydrological season. Because the second lidar survey occurred 30 days after the commencement of consistently positive air temperatures, and only 15 days after snow free conditions across the forefield, it was assumed minimal sediment entrainment occurred during early in 2005. To estimate total stream load a bedload contribution a value equivalent to 60% of the total suspended load was assumed: total load passing MLE during 2004 was 2560(±912) ×10$^3$kg. Compared to the mass indicated by the lidar analysis, this equates to only 64 to 85(±22)% of the mass redistribution suggested by the terrain difference model. While the associated uncertainties are large, the results suggest moraine density is overestimated: indicative of buried ice within the forefield.

Field observations confirmed exposures of buried ice along the newly occupied MLE reach (Figure 3b). However, the source and age of this ice remains undefined. Nonetheless, fluvial activity combined with buried ice has significant potential to result in accelerated morphological change with deglaciating forefields.

## 3.2     Exploration of Proglacial Subsurface Character

With suggestions of buried ice over the proglacial zone proximate to ML, and with previous research suggesting ice within glacier forefields is indeed common on Svalbard (e.g. Hambrey, 1984), it was necessary to place the results from the lidar models in a historical context and explore the distribution and extent of buried ice forms.

### 3.2.1     Long-term Forefield Terrain Change

Longer-term forefield change was estimated using DEMs with 10m horizontal resolution from 1966, 1977 and 1990, all constructed from photogrammetric methods, as detailed in Barrand et al. (2010). While it would be possible to compare the photogrammetrically derived DEMs to the more recent lidar data sets, algorithms involved in the DEM creation process mean that the DEMs may not be directly comparable: photogrammetric techniques invoke interpolation particularly in shadowed areas (missing data) resulting in elevation models exhibiting 'artificial' data and biased to illuminated highpoints within complex terrain, such as that found in glacial catchments (Hopkinson et al., 2009). For this reason direct comparison between lidar and photogrammetric DEMs was not undertaken.

Figure 4 illustrates the  terrain change between 1966 and 1990 for a profile over the western proglacial area (as

indicated in Figure 1). The results clearly show the glacier recession (see above) and, in isolating the proglacial area, suggest surface lowering rates along the profile of –0.20 ma$^{-1}$ between 1966 and 1977 and –0.13 ma$^{-1}$ from 1997 to 1990. Similar changes were observed throughout the proglacial area extending to the LIA moraine limit. When compared to the more recent lidar data, the profile showed a deceleration in the longer-term change rates to those derived for 2003-2005 (–0.06 ma$^{-1}$). Table 2 presents these change rate data within context. These data compare well to the rates evidenced by the lidar difference model, and serve as further evidence of buried ice at depth below the contemporary forefield surface.

Table 2. Long-term elevation changes (dZ) derived from the photogrammetric DEMs. Forefield sample data are taken as the average of 950 random points between the LIA moraine and the 1966 glacier margin.

| DEM difference | Uncertainty in dZ (m) | Mean glacier dZ (ma$^{-1}$) | Forefield sample dZ (ma$^{-1}$) |
|---|---|---|---|
| 1966-1977 | ±0.80 | –0.46 | –0.13 |
| 1977-1990 | ±0.84 | –0.37 | –0.02 |
| 2003-2005 | ±0.20 | –0.51 | –0.07 |

The long-term terrain change rates observed at ML appear to be slightly lower than those reported for forefield areas elsewhere in Svalbard (cf. Etzelmüller, 2000); it should be noted these other studies report greater uncertainties. However, the broad trend of terrain lowering is suggestive of spatially extensive thermal erosion rather than more discrete fluvial activity.

### 3.2.2     Process Identification

In order to verify the presence of buried ice, a resistivity survey was conducted across a number of profiles within the western forefield. Using a ABEM Terrameter SAS 300B, Hoelzle (1993) showed that resistivity surveys in the forefields of glaciers on Brøggerhalvøya successfully identified high resistivity buried ice concentrations. Here, an ABEM Terrameter System SAS 4000 with electrode spacing at 5 m intervals was used to plot subsurface resistivity between the LIA moraine limit and the contemporary glacier margin.

Figure 4 illustrates the provisional results from the resistivity survey for one of the profiles (as indicated on Figure 1). The interpretation of these results was that resistivity values greater than 8000 Ωm are suggestive of buried ice with overlying debris ranging from shallow (~ 1 m) to deep (> 5 m) across the . The buried ice itself would appear to have thicknesses of > 5 m.  Other profiles indicated buried ice masses are widespread across the western ML forefield. The overlying debris layer depths suggested by these surveys are similar to those elsewhere reported Brøggerhalvøya by Hoelzle (1993) using resistivity and by Brandt et al. (2007) using ground penetrating radar:  0.5 – 4 m  and  2 – 4 m,  respectively.
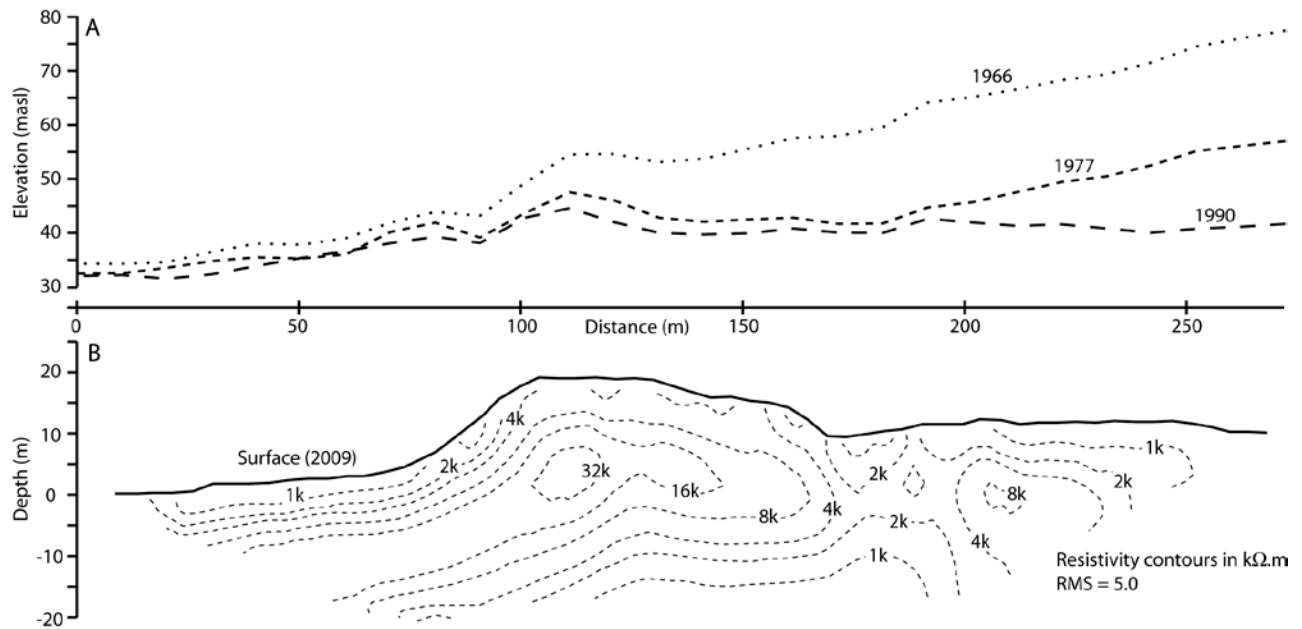
Figure 4. Plots for ML forefield profile P (see Figure 1) showing (A) surface change between 1966 and 1990 and (B) contour plot of the subsurface resistivity where ice is diagnosed with resistivity > 8kΩ.m.

Brandt et al (2007) also report buried ice bodies > 6 m in thickness within glacier forefields. Critically, however, the sediment mantle thickness is greater than the local active layer depth (1.5m), and exceeds the depth of ~ 2 m which is typically thought to effectively impede subsurface melting (Østrem, 1959). Therefore, to explain the longer-term topographic lowering identified using the DEM differencing analyses, a mechanism other than surface energy balance and conduction must be considered.

### 3.3 Identification of Periglacial Sediment Mobilisation

In a deglaciating catchment, however, the exposure of sediments to processes of reworking is not limited to the thermal erosion and fluvial action in glacial forefields. Previous field observations at AB and ML suggested debris flows do occur in ice marginal locations, even at higher elevations, and were most pronounced at AB where rates of glacier thinning have been greatest, exposing previously ice-covered detritus.

#### 3.3.1 Time Lapse Imaging

In order to confirm the process of sediment delivery to the ice surface from ice marginal debris flows, time lapse photography was undertaken in the upper reaches of AB (see Figure 5) with a Nikon Coolpix S550.

Imagery obtained from several sites shows that during the observation period, slow, downslope movement is continuous, but punctuated with localised higher magnitude movement events that have the capacity to move sediments to the ice surface and ultimately into the glacier hydrological system.

These processes are essentially analogs of retrogressive thaw slumps which occur in degrading

permafrost, or in response to active layer saturation. However, because the release of sediment is to the supraglacial environment, surface fluvial processes are likely to rework the debris over short time-frames, resulting in the potential for stochastic delivery of sediments to the glacier hydrological system.
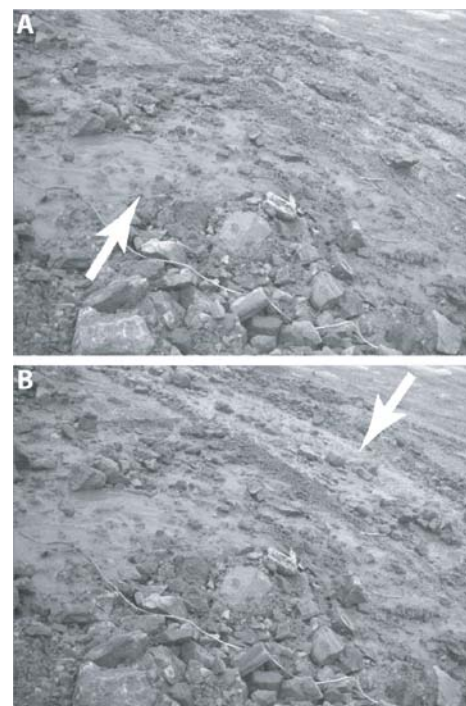


Figure 5. Example images from time-lapse series illustrating (A) slow, consistent debris flow and (B) rapid, stochastic thaw slump identified within image sequence.

1521

### 3.3.2 Sediment Transfer Identification

Because AB is a cold-based glacier, it has a distinctive hydrology which enables assessment of whether debris flows at the ice surface result in stochastic sediment pulses within streams emerging at the glacier margin. Previous analysis of AB's drainage system has shown that the majority of supraglacial meltwater is routed across the ice surface and through a number of moulins enters a coalescent englacial system. This englacial system emerges at a portal on the eastern ice margin (Figure 1) and direct observations (Vatne, 2001; unpublished) and geophysical surveying (Stuart et al., 2003) indicate that it is of the 'cut and closure' type described by Gulley et al. (2009). This englacial flowpath does not appear to contact the glacier bed at any location.

The suspended sediment concentration (SSC) in the meltwater emerging at the portal was monitored at high temporal resolution (2 min and 30 min) over a 5 day period using a Partech IR15C turbidity probe with a linear relationship between turbidity and SSC ($r^2$ = 0.9). Due to technical difficulties, the meltwater discharge at the portal was not recorded, necessitating the use of discharge records from 1 km downstream. Previous research has shown strong correlations between water discharge at the ice margin and in the downstream location: for example, during 2000, over an 86 day period the correlation coefficient (r) between ice marginal and downstream discharge records was greater than 80% with lag times < 30 mins (Hodson, unpublished data). The presence of permafrost limits any influence by groundwater inputs. Thus the downstream record was assumed to be representative of the discharge emerging from the portal (Figure 5).

Visually, 15 peaks in turbidity which appeared unrelated to discharge (Q) were observed with a maximum SSC of ~ 0.85 gl$^{-1}$. To confirm the presence of these stochastic sediment pulses, a Fourier transform was applied to the turbidity and Q records. Low, medium and high pass filters applied in the frequency domain were used to decompose the time-series into three components: > 2 days, 0.5 – 2 days and < 0.5 days. Data resampled at either 2 min or 30 min resolution yielded the same result. Figure 6 plots the turbidity signal against Q signal for the three timescales. The broadly positive associations at timescales > 0.5 days illustrate the discharge forcing of SSC, with evidence of hysteresis at the diurnal scale as has been observed previously for the same drainage system (Hodson et al., 1998). The lack of association between turbidity and Q at the < 0.5 day timescale implied the presence of stochastic turbidity pulses. Because of the absence of a subglacial drainage system at AB, the source of such pulses must be within the englacial channel or from the supraglacial environment. Observations indicate that debris within the englacial channel consists of coarse sediments, indicative of a supraglacial origin (e.g. rockfall), and so are unlikely to provision the fine sediment for suspended transport (Vatne, 2001). The interpretation here is that the debris flow slumps observed with time-lapse photography are the source of the stochastic turbidity pulses as the sediments exposed at the ice margins have a typically high fine content and turbid surpaglacial streams were observed to originate close to locations of observed debris slumps.
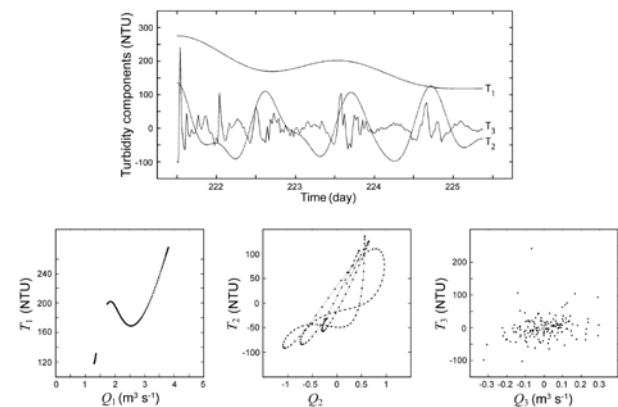


Figure 6. Decomposition of SSC (turbidity) time-series by high, mid and low pass filters showing broadly positive correlations between Q and SSC for diurnal or longer cycles and absence of association between variables at cycles less than 12hrs in duration.

Lukas et al (2005) suggested that during summer thaw on Svalbard, local debris flow processes on exposed till faces may liberate $5 \times 10^3$kg of sediment per day. Isolation of individual sediment pulses from the turbidity record at AB demonstrate that between 30% and 45% (approximately $4 \times 10^3$kg per day) of the sediment yield from the portal's catchment is delivered during transient periods of elevated suspended sediment load. And, assuming a simple bivariate relation between Q and SSC (r > 0.7), it is estimated the flow processes themselves provide > 5% of the total sediment yield. If, as suggested here, these sediment pulses originate from debris flow slumps in the upper reaches, then these observations reiterate the importance of the linkages between glacial, periglacial and fluvial processes in terms of the sediment cascade within deglaciating Arctic catchments (e.g. Etzelmüller and Hagen, 2005).

## 4 DISCUSSION

In combining the findings presented above, the key association identified is the glacier-permafrost interaction which appears characteristic of contemporary Arctic proglacial and ice-marginal areas.

It has been suggested that ice dynamics within polythermal glaciers may enable transport of debris from subglacial to supraglacial locations, which once deposited may protect underlying ice from ablation in permafrost conditions (Hoelzle, 1993) while for cold glaciers, the stagnating ice may promote the meltout of englacial debris which may similarly accumulate on the descending surface (Lukas et al., 2005). It is assumed that in a permafrost environment where debris thicknesses greater than climatically defined active layer leads to protection of underlying ice (Etzelmüller and Hagen, 2005) and permafrost would be expected to aggrade with glacier

recession (Kniesel, 2003). For glaciers in Svalbard retreating from their LIA maxima, Hambrey (1984) asserted progressively exposed proglacial areas are likely to be underlain by stagnant ice of unknown thickness. Here, in a permafrost region, while confirming the presence of spatially extensive buried ice forms, these forms are shown to be currently unstable.

The degradation of ML's ice-cored moraine shows the landform is in disequilibrium with the contemporary climate, and subject to thermal erosion. Importantly, exposure of the moraine's ice-core by periglacial thaw slumps or by fluvial action accelerates the feature's decay (cf. Lukas et al., 2005; Moorman, 2005). Similarly, it is fluvial incision which enables the rapid degradation of buried ice forms within the forefield, which should in the permafrost environment be stable features.

At ML, the forefield terrain change identified since 1966 implies two possible degradation mechanisms. The first is periglacial slope processes coupled with fluvial activity, the second is the degradation of buried ice. From the DEM analysis it would seem morphometric change is relatively small and a simple vertical relaxation of the terrain appears more descriptive of the change. This would implicate the decay of the buried ice. Hambrey (1984) suggested that despite active glacier margins appearing well-defined, dead (buried) ice may remain within forefield sediments and while dynamically isolated from the main glacier body can remain hydrologically linked to en- or subglacial drainage systems. Such glacial-periglacial hydrological connections have been observed for polythermal glaciers in the Canadian Arctic (Moorman, 2005; Moorman and Michel, 2000), and the thermal significance of these structures may at least partially explain subsurface degradation and lowering of deglaciating surface topography (e.g. Clayton, 1964).

The processes of moraine and forefield degradation support the notion of permafrost as a regulator of material availability by reducing the likelihood of sediment exhaustion. Despite the low erosion potential of catchments in permafrost regions, such catchments can have high material transport rates (Etzelmüller and Hagen, 2005) as exemplified here with the degradation forefield terrain by coupled periglacial and fluvial processes. However, these sources and transfers of sediment may be accentuated by the increase in sediment availability at the ice margin. The interactions between glacial and periglacial processes are shown to accentuate sediment yields as a byproduct of retrogressive thaw slumps occurring where glacier thinning exposes readily destabilized material at the ice-margin, even at higher elevations. Combined, rather than glacial sources, the redeposition and remobilization of sediments in the forefield and at the ice-margin may promote enhanced sediment aggradation in coastal (fjord) environments (Mercier and Laffly, 2005). Thus the observations presented here support the argument that sediment flux from terrestrial Svalbard was greatest during interstadials and interglacials when periglacial and fluvial processes result in efficient reworking and transport of sediments from deglaciating catchments (Elverhøi et al., 1995). As Everest and Bradwell (2003) discuss, deglaciation should be considered as a two-stage process: that of active glacier retreat and then the subsequent decay of stagnant, buried ice forms.

## 5    CONCLUSION

Analyses of terrain change and identification of buried ice phenomena and periglacial (thaw) processes exemplify the interaction between glacial and periglacial conditions which strongly condition both the timing and manner in which the sedimentary morphology of a deglaciating catchment in the Arctic changes. The results here show how hydrological and fluvial processes may be progressively important and the most critical to both rapid and longer-term forefield change in a permafrost environment. The morphological dynamics of forefield terrain through the ablation of buried ice may lead to the development of sedimentary structures which are indistinguishable from non-glacial processes. Thus, interpretation of forefield landforms, particularly in permafrost settings, is potentially problematic. Critically, the glacial-periglacial interactions are key parameters determining the rates of proglacial and ice-marginal terrain change following deglaciation in the Arctic, and these processes and rates may have significant impacts upon the temporal signature of sediment yield from partially glacierised catchments.

## 6    BIBLIOGRAPHY

Barrand, N.E., James, T.D. and Murray, T., 2010. Spatiotemporal variability in elevation changes of two high-Arctic valley glaciers. *Journal of Glaciology*.

Barrand, N.E., Murray, T., James, T.D., Barr, S.L. and Mills, J.P., 2009. Optimizing photogrammetric DEMs for glacier volume change assessment using laser-scanning derived ground control points. *Journal of Glaciology*, 55(189): 103-116.

Björnsson, H., Gjessing, Y., Hamran, S.-E., Hagen, J.O., Liestøl, O., Pálsson, F. and Erlingsson, B., 1996. The thermal regime of sub-polar glaciers mapped by multi-frequency radio-echo sounding. *Journal of Glaciology*, 42(140): 23-32.

Brandt, O., Langley, K., Kohler, J. and Hamran, S.-E., 2007. Detection of buried ice and sediment layers in permafrost using multi-frequency Ground Penetrating Radar: a case examination on Svalbard. *Remote Sensing of Environment*, 111: 212-227.

Clayton, L., 1964. Karst topography on stagnant glaciers. *Journal of Glaciology*, 5(37): 107-112.

Elverhøi, A., Svendsen, J.I., Solheim, A., Andersen, E.S., Milliman, J., Mangerud, J. and Hooke, R.L., 1995. Late Quaternary sediment yield from the high arctic Svalbard area. *Journal of Geology*, 103: 1-17.

Etzelmüller, B., 2000. Quantification of thermo-erosion in proglacial areas - examples from Svalbard. *Zeitschrift fur Geomorphologie*, 44: 343-361.

Etzelmüller, B. and Hagen, J.O., 2005. Glacier-permafrost interaction in Arctic and alpine mountain environments with examples from southern Norway and Svalbard. In: C. Harris and J. Murton (Editors), Cryospheric Systems: Glaciers and Permafrost. Geological Society Special Publication, London, pp. 11-27.

Etzelmüller, B., Ødegård, R.S., Vatne, G., Mysterud, R.S., Tonning, T. and Sollid, J.L., 2000. Glacial characteristics and sediment transfer system of Longyearbreen and Larsbreen, western Spitsbergen. *Norsk Geografisk Tidsskrift*, 54: 157-168.

Everest, J. and Bradwell, T., 2003. Buried glacier ice in southern Iceland and its wider significance. *Geomorphology*, 52: 347-358. DOI:10.1016/S0169-555X(02)00277-5.

Førland, E.J., Hanssen-Bauer, I. and Nordli, P.Ø., 1997. Climate statistics and longterm series of temperature and precipitation at Svalbard and Jan Mayen. DNMI Klima Report 21/97, Oslo.

Gibas, J., Rachlewicz, G. and Szczucinski, W., 2005. Application of DC resistivity soundings and geomorphological surveys in studies of modern Arctic glacier marginal zones, Petuniabukta, Spitsbergen. *Polish Polar Research*, 26(4): 239-258.

Glasser, N.F. and Hambrey, M.J., 2001. Styles of sedimentation beneath Svalbard valley glaciers under changing dynamic and thermal regimes. *Journal of the Geological Society*, 158: 697- 707.

Gulley, J., Benn, D.I., Luckman, A. and Müller, D. 2009. A cut-and-closure origin for englacial conduits on uncrevassed parts of polythermal glaciers. *Journal of Glaciology* 55 (189), 66-80.

Hagen, J.O., Liestøl, O., Roland, E. and Jørgensen, T., 1993. Glacier Atlas of Svalbard and Jan Mayen. Meddelelser 129. Norsk Polarinstitutt, Olso.

Hallet, B. and Prestrud, S., 1986. Dynamics of periglacial sorted circles in western Spitsbergen. *Quaternary Research*, 26: 81-99.

Hambrey, M.J., 1984. Sedimentary processes and buried ice phenomena in the proglacial areas of Spitsbergen glaciers. *Journal of Glaciology*, 30: 116-119.

Hjelle, A., Piepjohn, K., Saalmann, K., Ohta, Y., Thiedig, F., Salvigsen, O. and Dallmann, W.K., 1999. Geological map of Svalbard 1:100,000 (A7G Kongsfjorden), Norsk Polarinstitutt Temakart (30). Norwegian Polar Institute, Tromsø.

Hodson, A., Gurnell, A., Tranter, M., Bogen, J., Hagen, J.O. and Clark, M., 1998. Suspended sediment yield and transfer processes in a small High-Artic glacier basin, Svalbard. *Hydrological Processes*, 12(1): 73-86.

Hodson, A., Tranter, M., Gurnell, A., Clark, M. and Hagen, J.O., 2002. The hydrochemistry of Bayelva, a high Arctic proglacial stream in Svalbard. *Journal of Hydrology*, 257(1-4): 91-114.

Hodson, A.J. and Ferguson, R.I., 1999. Fluvial suspended sediment transport from cold and warm-based glaciers in Svalbard. *Earth Surface Processes and Landforms*, 24(11): 957-974.

Hoelzle, M., 1993. DC resistivity soundings 1992 in north-western Svalbard. Arbeitsheft Nr. 13, Versuchsanstalt für Wasserbau. ETH, Zürich, Switzerland, 37 pp.

Hopkinson, C., Hayashi, M. and Peddle, D., 2009. Comparing alpine watershed attributed from LiDAR, photogrammetric, and contour-based digital elevation models. *Hydrological Processes*, 23: 451-463. DOI: 10.1002/hyp.7155.

Kniesel, C., 2003. Permafrost in recently deglaciated glacier forefield - measurements an observations in the eastern Swiss Alps and norther Sweden. *Zeitschrift fur Geomorphologie*, 47(3): 289-305.

Kohler, J., James, T.D., Murray, T., Nuth, C., Brandt, O., Barrand, N.E., Aas, H.F. and Luckman, A., 2007. Acceleration in thinning rate on western Svalbard glaciers. *Geophysical Research Letters*, 34(L18502): 5 pp. doi:10.1029/2007GL030681.

Liestøl, O., 1976. Pingos, springs and permafrost in Spitsbergen. Norsk Polarinstitutt Årbok, 1975, 7-29 pp.

Lønne, I. and Lyså, A., 2005. Deglaciation dynamics following the Little Ice Age on Svalbard: implications for shaping of landscapes at high latitudes. *Geomorphology*, 72: 300-319. doi:10.1016/j.geomorph.2005.06.003.

Lukas, S., Nicholson, L.I., Ross, F.H. and Humlum, O., 2005. Formation, meltout processes and landscape alteration of High-Arctic ice-cored moraines - examples from Nordenskiöld Land, central Spitsbergen. *Polar Geography*, 29(3): 157-187.

Mercier, D. and Laffly, D., 2005. Actual paraglacial progradation of the coastal zone in the Kongsfjorden area, western Spitsbergen (Svalbard). In: C. Harris and J. Murton (Editors), Cryospheric Systems: Glaciers and Permafrost. Geological Society Special Publication, London, pp. 111-117.

Moorman, B.J., 2005. Glacier-permafrost hydrological interconnectivity: Stagnation Glacier, Bylot Island, Canada. In: C. Harris and J. Murton (Editors), Cryospheric Systems: Glaciers and Permafrost. Geological Society Special Publication, London, pp. 63-74.

Moorman, B.J. and Michel, F.A., 2000. The burial of ice in the proglacial environment on Bylot Island, Arctic Canada. *Permafrsot and Periglacial Processes*, 11: 161-175.

Moreau, M., Mercier, D., Laffly, D. and Roussel, E., 2008. Impacts of recent paraglacial dynamics on plant colonization: a c ase study on Midtre Lovénbreen forefield, Spitsbergen (79°N). *Geomorphology*, 95: 48-60. doi:10.1016/j.geomorph.2006.07.031.

Nuth, C., Kohler, J., Aas, H.F., Brandt, O. and Hagen, J.O., 2007. Glacier geometry and elevation changes on Svalbard (1936-90): a baseline dataset. *Annals of Glaciology*, 46: 106-116.

Østrem, G., 1959. Ice metling under a thin layer of moraine, and the existence of ice cores in moraine ridges. *Geografiska Annaler*, 41: 228-320.

Rippin, D., Willis, I., Arnold, N., Hodson, A., Moore, J., Kohler, J. and Bjornsson, H., 2003. Changes in geometry and subglacial drainage of Midre Lovenbreen, Svalbard, determined from digital elevation models. *Earth Surface Processes and Landforms*, 28(3): 273-298. doi: 10.1002/esp.485.

Schomacker, A. and Kjær, K.H., 2008. Quantification of dead-ice melting in ice-cored moraines at the high-Arctic glacier Holmströmbreen, Svalbard. *Boreas*, 37: 211-225. DOI: 10.1111/j.1502–3885.2007.00014.x.

Stuart, G., Murray, T., Gamble, N., Hayes, K. and Hodson, A., 2003. Characterization of englacial channels by ground-penetrating radar: An example from austre Broggerbreen, Svalbard. *Journal of Geophysical Research-Solid Earth*, 108(B11, 2525): 13 pp. doi:10.1029/2003JB002435.

Svendsen, H., Beszczynska-Moller, A., Hagen, J.O., Lefauconnier, B., Tverberg, V., Gerland, S., Orbaek, J.B., Bischof, K., Papucci, C., Zajaczkowski, M., Azzolini, R., Bruland, O., Wiencke, C., Winther, J.G. and Dallmann, W., 2002. The physical environment of Kongsfjorden-Krossfjorden, an Arctic fjord system in Svalbard. *Polar Research*, 21(1): 133-166.

Svendsen, J.I. and Mangerud, J., 1997. Holocene glacial and climatic variations on Spitsbergen, Svalbard. *The Holocene*, 7(1): 45-57.

Vatne, G., 2001. Geometry of englacial water conduits, Austre Brøggerbreen, Svalbard. *Norsk Geografisk Tidsskrift*, 55: 24-33.

Ziaja, W., 2001. Glaicer recession in Sørkappland and central Nordenskiöldland, Sptisbergen, Svalbard, during the 20th century. *Arctic Antarctic and Alpine Research*, 33(1): 36-41.